Electronic Supplementary Material (ESI) for Nanoscale Horizons.

– Supporting Information –

Giant Enhancement of Initial SERS Activity for Plasmonic Nanostructures *via* Pyroelectric PMN-PT

Mingrui Shao[a], Di Liu[b], Jinxuan Lu[a], Xiaofei Zhao[a], Jing Yu[a], Chao Zhang[a], Baoyuan Man[a,*], Hui Pan[b,c,*], and Zhen Li[a,*]

[a] School of Physics and Electronics, Shandong Normal University, Jinan 250014, China

[b] Institute of Applied Physics and Materials Engineering, University of Macau, Macao SAR, 999078, P.R. China

[c] Department of Physics and Chemistry, Faculty of Science and Technology, University of Macau, Macao SAR, 999078, P. R. China

[*] Corresponding Authors: byman@sdnu.edu.cn, huipan@um.edu.mo, and lizhen19910528@163.com

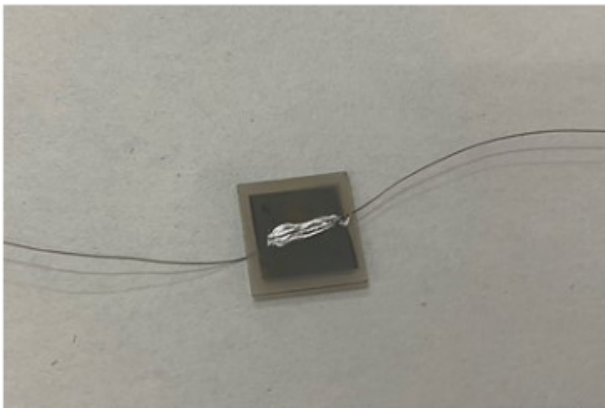

Figure S1. Optical photograph of gold-wired sample used for electrical experiments.

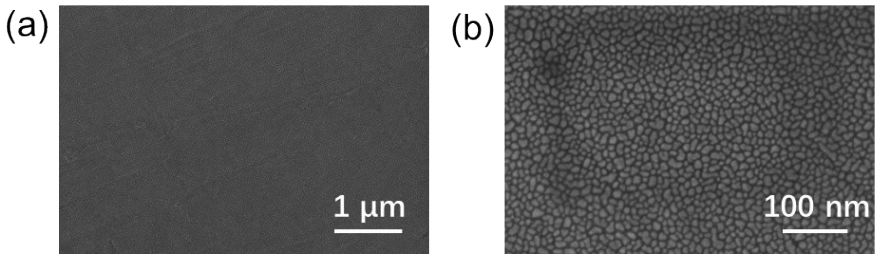

Figure S2. (a) and (b) SEM images of the prepared PMN-PT/Ag NP substrate at different magnifications.

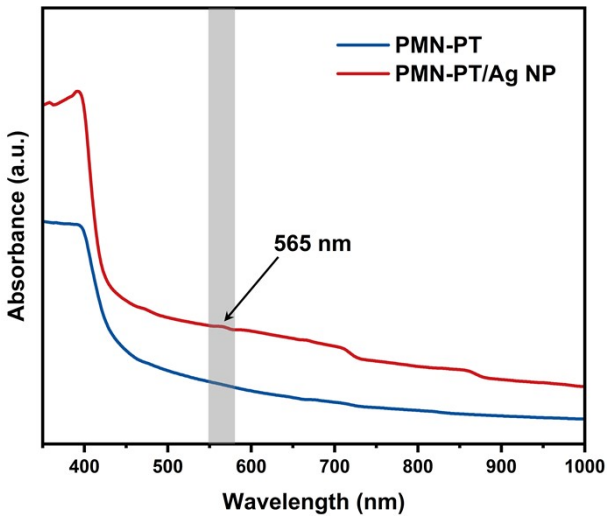

Figure S3. UV-vis-NIR spectra of the PMN-PT and PMN-PT/Ag NP substrates.

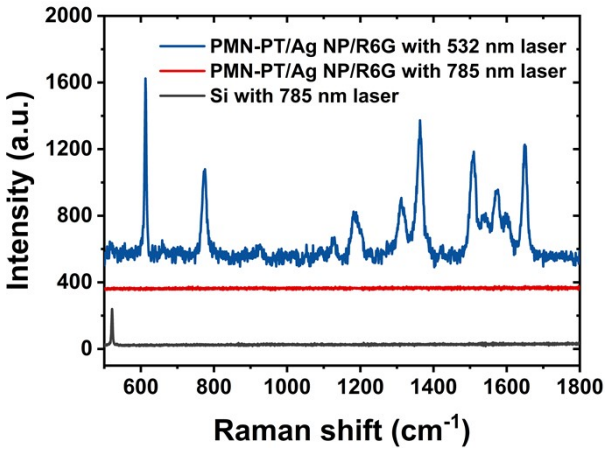

Figure S4. SERS spectra of R6G (10^{-5} M) on PMN-PT/Ag NP substrate irradiated by 532 or 785 nm laser as well as Raman spectra of silicon wafer irradiated by 785 nm laser.

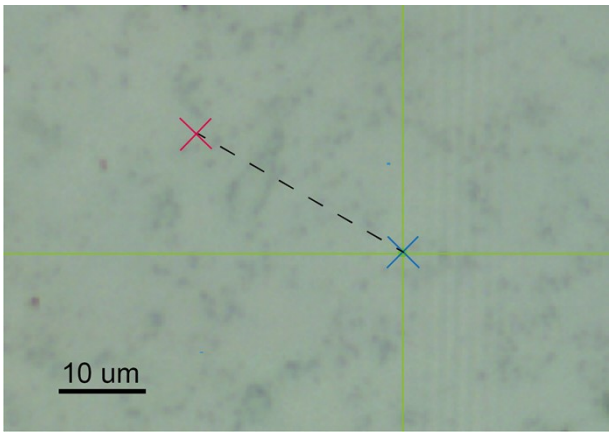

Figure S5. The optical microscopic image of PMN-PT/Ag NP. At 20 ℃, the laser spot is located at the blue cross line, and as the temperature increased to 100 ℃, the laser spot moved to the red cross line.

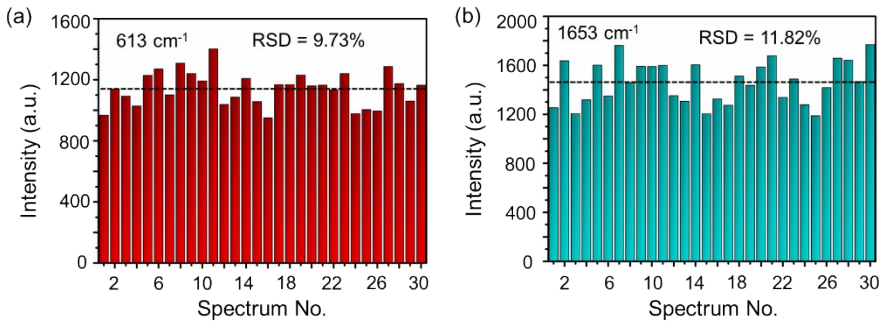

Figure S6. Raman mapping of R6G (10^{-5} M) adsorbed on the PMN-PT/Ag NP substrate at 613 cm^{-1} (a) and 1653 cm^{-1} (b).

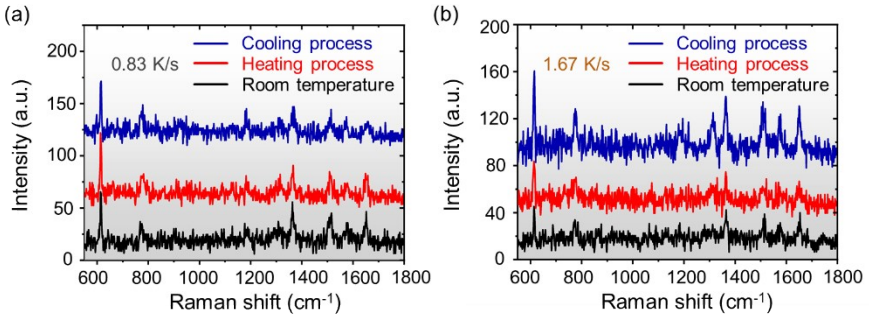

Figure S7. SERS spectra of R6G (10^{-7} M) obtained at 0.83 ℃/s (a) and 1.67 ℃/s (b), respectively.

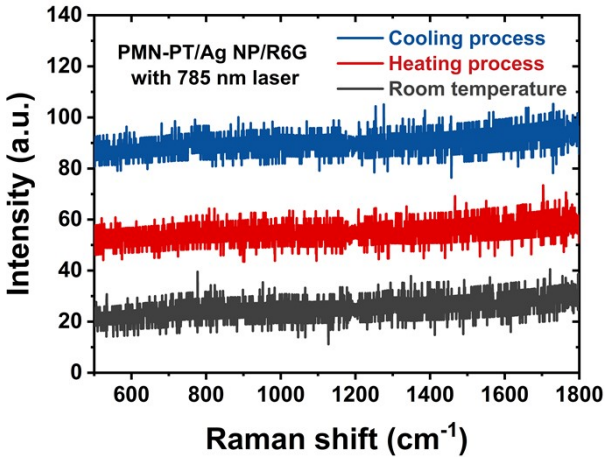

Figure S8. SERS spectra of R6G (10^{-5} M) on PMN-PT/Ag NP substrate under 785 nm laser irradiation. The temperature change rate is 2.5 ℃/s.

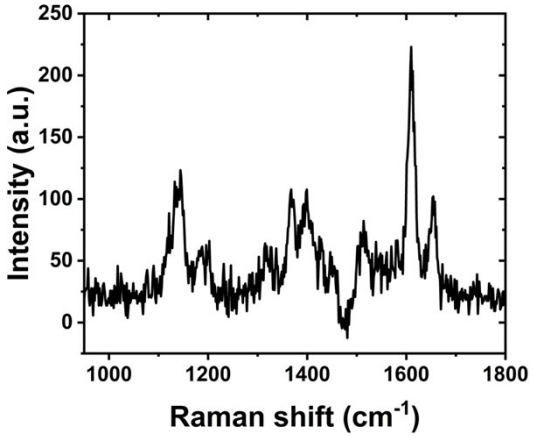

Figure S9. SERS spectra of MO (10^{-7} M) on PMN-PT/Ag NP substrate at room temperature.

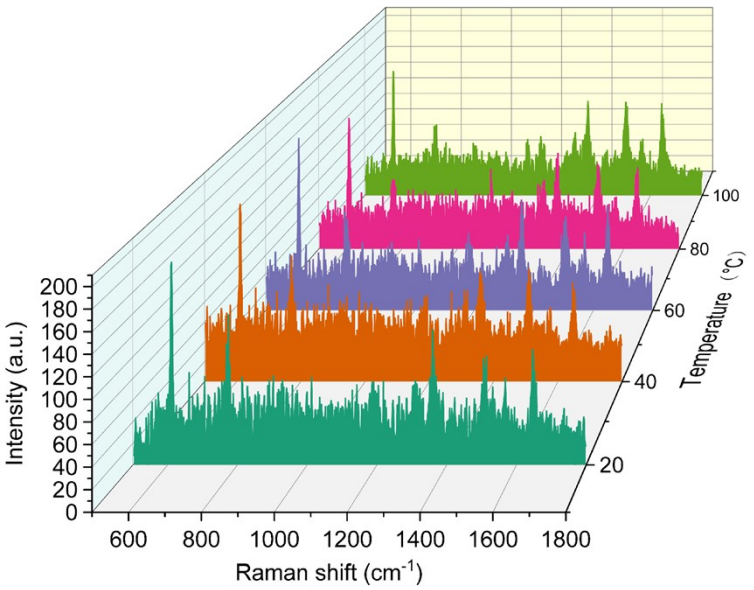

Figure S10. SERS spectra of R6G (10^{-7} M) on PMN-PT/Ag NP substrate at 20, 40, 60, 80 and 100 ℃, respectively.

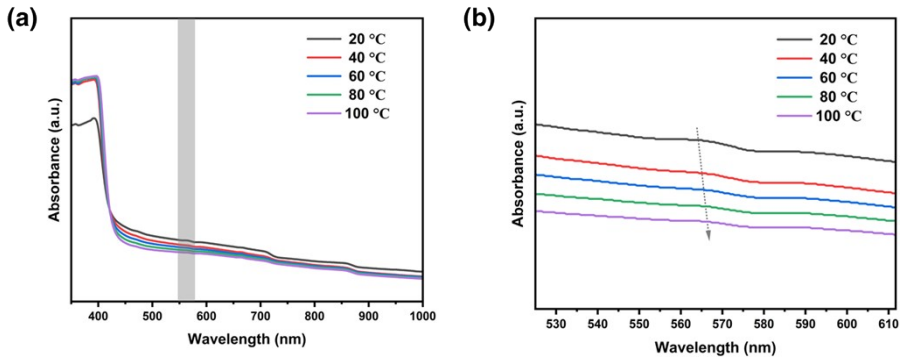

Figure S11. Temperature-dependent UV-vis-NIR spectra of PMN-PT/Ag NP substrate.

As shown in Fig. S9, the LSPR peak of Ag NPs is slightly redshifted with the increase of temperature. This result can be understood by the following formula:[1]

$$\omega_{LSPR} \propto \omega_p = \sqrt{\frac{N_e e^2}{m^* \varepsilon_0}}$$

in which m^* refers to the effective mass of the carrier, e is the charge of an electron and ε_0 represents the vacuum permittivity. The LSPR frequency (ω_{LSPR}) is proportional to the plasma frequency (ω_p), which in turn is proportional to the square root of the carrier density. When the temperature of the substrate increases, the spontaneous polarization of PMN-PT becomes weak, which leads to the decrease of carrier density on the Ag NPs surface, and then causes the redshift of LSPR peak.

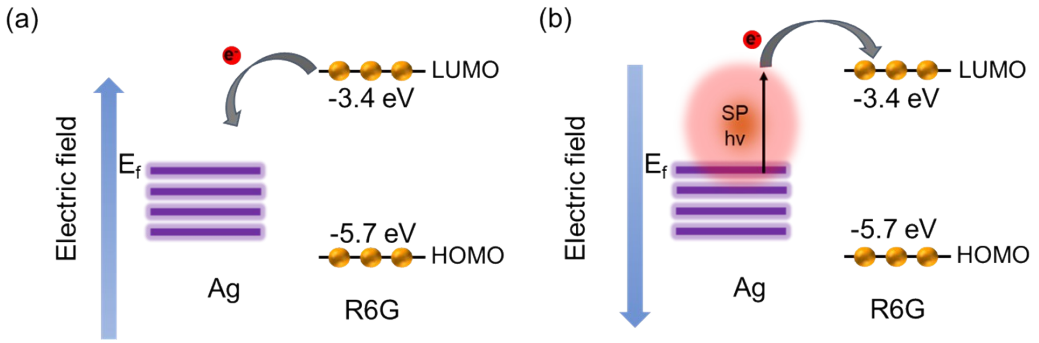

Figure S12. (a) Schematic diagram of electron transfer of R6G-Ag system when an upward electric field is applied. (b) Schematic diagram of electron transfer of R6G-Ag system when a downward electric field is applied.

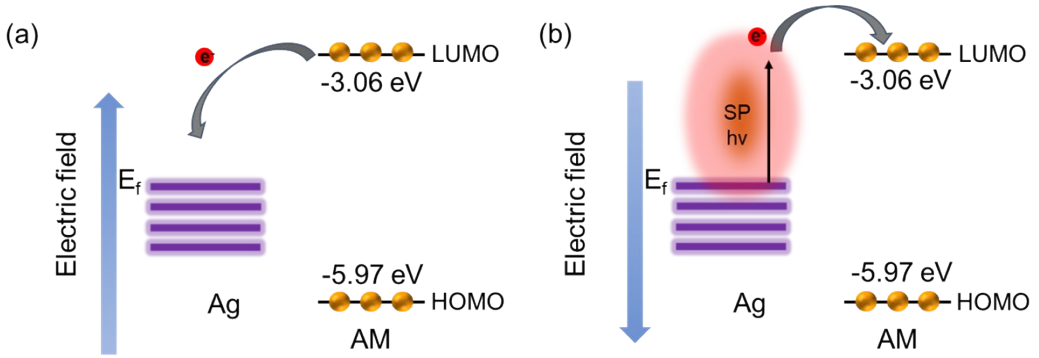

Figure S13. (a) Schematic diagram of electron transfer of AM-Ag system when an upward electric field is applied. (b) Schematic diagram of electron transfer of AM-Ag system when a downward electric field is applied.

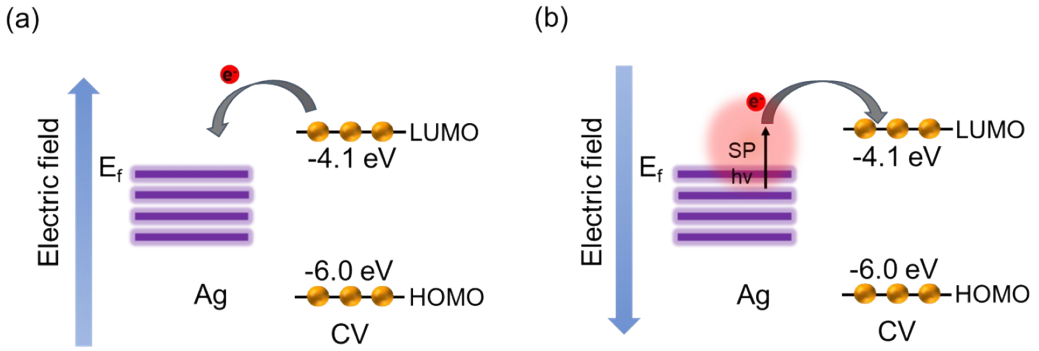

Figure S14. (a) Schematic diagram of electron transfer of CV-Ag system when an upward electric field is applied. (b) Schematic diagram of electron transfer of CV-Ag system when a downward electric field is applied.

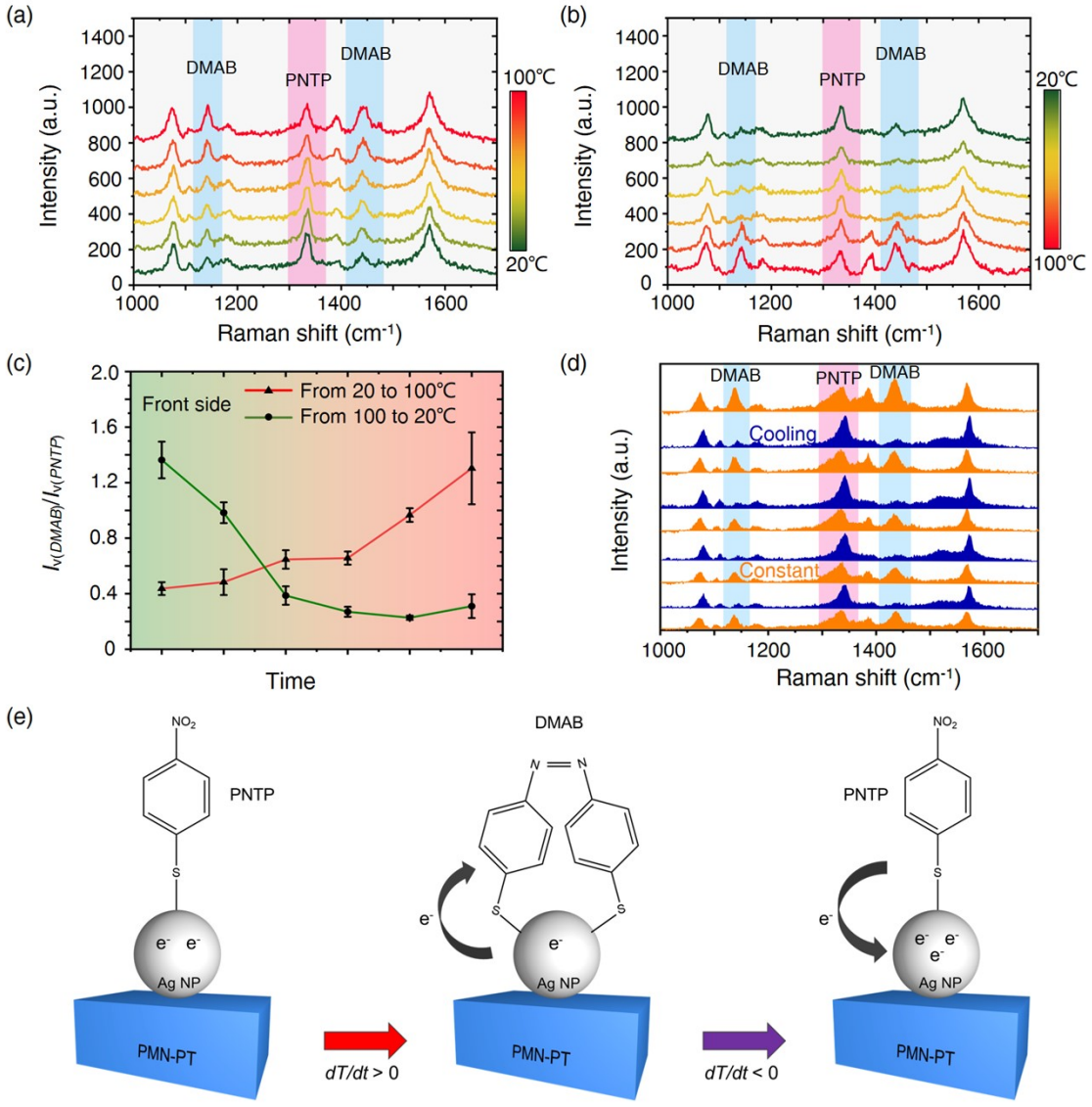

Figure S15. The dynamic SERS spectra of PNTP on PMN-PT/Ag NP under heating (a) and cooling (b). (c) The dynamic changes in the value of $I_{(1445\ cm^{-1})}/I_{(1334\ cm^{-1})}$ on PMN-PT/Ag NP under heating (red line) and cooling (greed line). (d) SERS spectra collected under cooling (purple) and constant (orange) conditions. (e) Schematic diagram of electron migration between Ag NP and adsorption molecule.

Efficient catalysis in redox reactions is required in industrial processes. Plasmonic metal nanoparticles with high catalytic activity and tunability are promising materials in catalysis due to

abundant photoexcited hot electrons from LSPR. In addition, the SERS signal can also be generated in the area where hot electrons appear, which makes the real-time monitoring of the catalytic process triggered by hot electrons very promising. However, there is still a lack of understanding of the hot electrons transfer process at the plasmonic metal interface and how it affects photocatalysis. As a typical plasmon-driven chemical reaction, the photocatalytic transition between PNTP and DMAB can effectively reflect the plasmon activity of SERS substrates. We investigated the impact of heating and cooling PMN-PT/Ag NP on the reduction of *p*-nitrothiophenol (PNTP) to *p*,*p*'-dimercaptoazobenzene (DMAB). As shown in Fig. S15a, the spectrum shows a strong 1334 cm^{-1} characteristic band at the initial 20 °C, which is attributed to the NO_2 stretching mode of PNTP. However, the intensities of two new vibrational modes at 1145 and 1445 cm^{-1} gradually increase as rising temperature, indicating the formation of DMAB. [2-4] It is worth noting that when the temperature of PMN-PT/Ag NP drops, the intensities of the DMAB characteristic bands are significantly reduced (Fig. S15b). Therefore, we conclude that DMAB is converted back to PNTP during the cooling process. The value of $I_{(1445\ cm^{-1})}/I_{(1334\ cm^{-1})}$ can be used to characterize the degree for the conversion of PNTP to DMAB. During the heating process, the ratio increases continuously, while during the cooling process, this ratio decreases rapidly, presenting two completely different trends (Fig. S15c). In the end (green line), the value of $I_{(1445\ cm^{-1})}/I_{(1334\ cm^{-1})}$ tends to rise again because the sample temperature remains stable after the cooling. In order to validate the necessity of the cooling process for DMAB to be converted back to PNTP, we compared the SERS spectra collected under cooling and constant conditions, as shown in Fig. S15d. The Raman peaks of DMAB in the former (blue in Fig. S15d) can be scarcely observed, while the latter (orange in Fig. S15d) shows high DMAB peaks, suggesting that a continuous cooling process is indispensable for the conversion of DMAB to PNTP. Previous study has revealed that the conversion between PNTP and DMAB is entirely reversible under the applied electric field.[5] Our experimental results show that reversal electron transfer can occur between Ag and adsorbed molecules with the rise or drop of the temperature.

When the temperature rises, a downward electric field appears on the surface of PMN-PT/Ag NP, resulting in the easier transfer of electrons to PNTP, then PNTP is dimerized into DMAB by the reduction reaction. Furthermore, an upward electric field appears when the temperature drops, inducing more electrons in Ag NPs, which participate in the activation step of oxygen (O_2) in air to generate superoxide anions (O_2^-), thus oxidizing DMAB to PNTP (Fig. S15e).[6] We also performed a contrast test on the other side of PMN-PT/Ag NP. The trend of $I_{(1445\ cm^{-1})}/I_{(1334\ cm^{-1})}$ value changing with temperature is contrary to the above study (Fig. S16), which is consistent with the analysis on PMN-PT/Ag NP. In a nutshell, multiple dimerization of PNTP and back conversion can be realized by controlling temperature change.

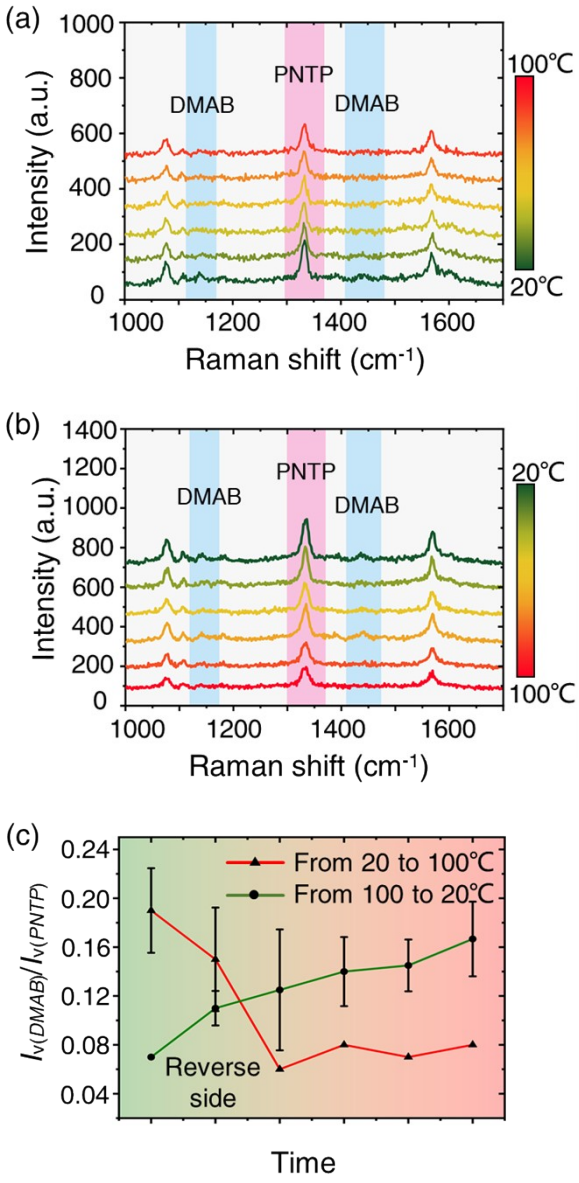

Figure S16. The dynamic SERS spectra of PNTP adsorbed on the other side of PMN-PT/Ag NP during heating (a) and cooling (b). (c) The dynamic changes in value of $I_{(1445\ cm^{-1})}/I_{(1334\ cm^{-1})}$ as PMN-PT/Ag NP was heated (red line) and cooled (greed line).

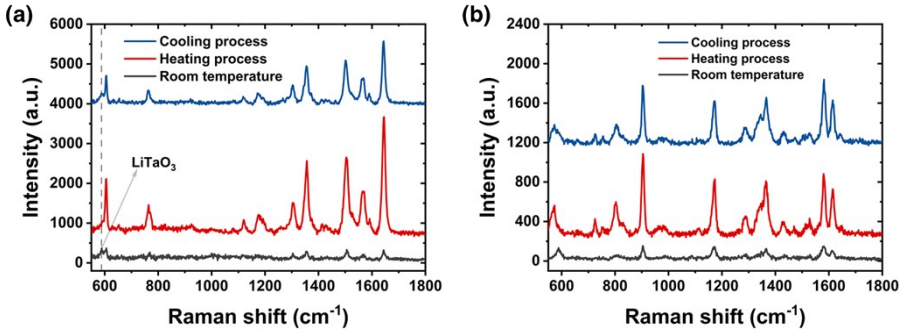

Figure S17. SERS spectra recorded at RT and variable temperature from 20 ℃ (100 ℃) to 100 ℃ (20 ℃) at a rate of 2.5 ℃/s for (a) R6G (10^{-7} M) and (b) CV (10^{-7} M) on $LiTaO_3$/Ag NP substrate.

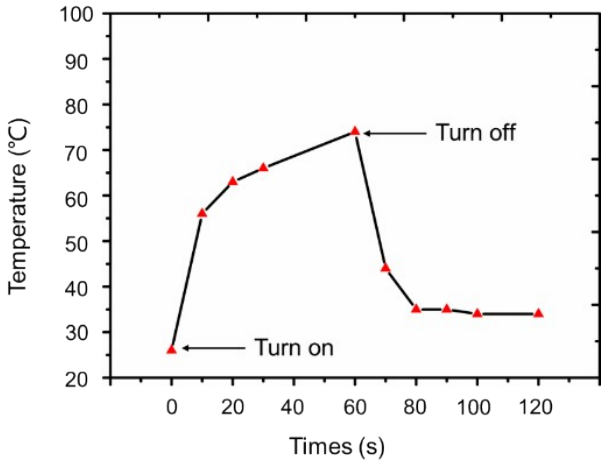

Figure S18. The maximum temperature of PMN-PT/Ag/Al_2O_3/Ag NC with time after the simulated sunlight is turned on and off.

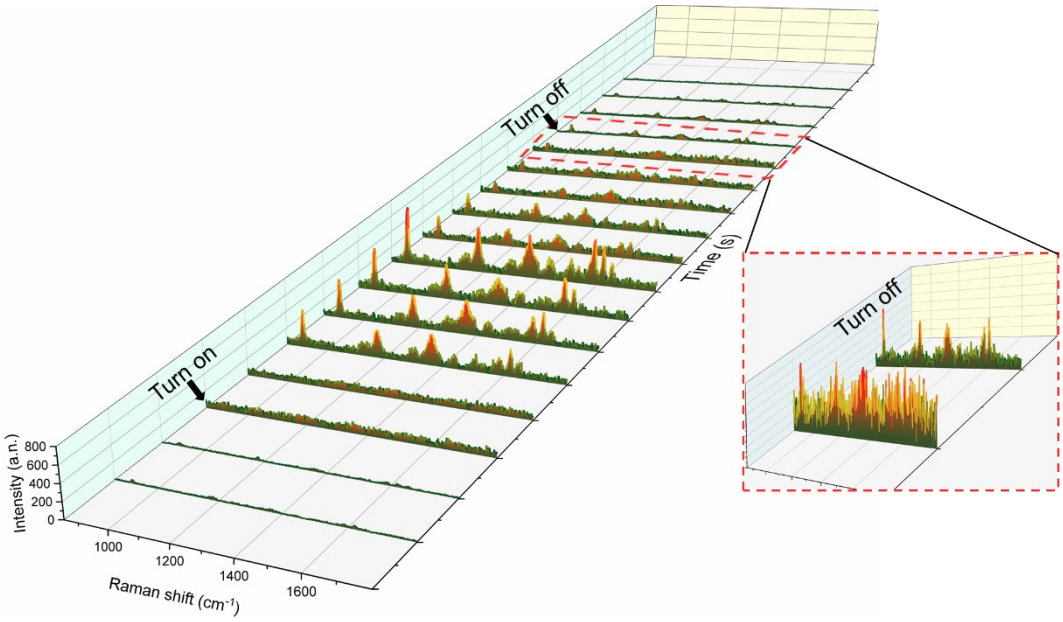

Figure S19. The time-dependent SERS spectra of CV (10^{-7} M) on PMN-PT/Ag/Al_2O_3/Ag NC after the simulated sunlight is turned on and off.

Table S1. Enhancement details of several typical characteristic peaks of R6G and MO molecules.

Molecular	Raman shift (cm^{-1})	Intensity (a.u.) (RT)	Intensity (a.u.) (HP)	Intensity (a.u.) (CP)	Magnification (HP)	Magnification (CP)
R6G	613	230	1432	3599	6.2	15.6
	1653	115	1212	3074	10.5	26.7
MO	1144	67	579	5244	8.6	78.2
	1426	31	410	3853	13.2	124.2

References

1 B. B. Han, L. Chen, S. Jin, S. Guo, J. M. Park, H. S. Yoo, J. H. Park, B. Zhao, and Y. M. Jung, *J. Phys. Chem. Lett.*, 2021, **12**, 7612-7618.

2 X. W. Xiu, L. P. Hou, J. Yu, S. Z. Jiang, C. H. Li, X. F. Zhao, Q. Q. Peng, S. Qiu, C. Zhang, B. Y. Man, and Z. Li, *Nanophotonics*, 2021, **10**, 1529.
3 M. T. Sun, and H. X. Xu, *Small*, 2012, **8**, 2777.
4 E. Cao, X. Guo, L. Q. Zhang, Y. Shi, W. H. Lin, X. C. Liu, Y. R. Fang, L. Y. Zhou, Y. H. Sun, Y. Z. Song, W. J. Liang, and M. T. Sun, *Adv. Mater. Interfaces*, 2017, **4**, 1700869.
5 S. Almohammed, S. T. Barwich, A. K. Mitchell, B. J. Rodriguez, and J. H. Rice, *Nat. Commun.*, 2019, **10***,* 2496.
6 J. L. Wang, R. A. Ando, and P. H. C. Camargo, *Angew. Chem., Int. Ed.*, 2015, **54**, 6909.